RSC Advances

PAPER

View Article Online
View Journal | View Issue

Cite this: *RSC Adv.*, 2024, **14**, 7932

Green synthesis of cadmium oxide nanoparticles (CdO-NPS) using syzygium cumini: exploring industrial applications of CdO NPs as a corrosion inhibitor of mild steel in the acidic environment

Sivakumar Sivalingam, *[a] Jyoti Kavirajwar,[b] K. Seethalakshmi,[c] Jayagopi Gayathri*[a] and A. Roniboss[a]

Received 22nd January 2024
Accepted 27th January 2024

DOI: 10.1039/d4ra00560k

rsc.li/rsc-advances

Potentiodynamic polarization (PDP), electrochemical impedance spectroscopy (EIS) and weight loss measurements were used to assess the effectiveness of CdO-NPs as a corrosion inhibitor for carbon steel in 0.5 M H_2SO_4. It was amply shown that as the concentration of CdO-NPs increased, the cathodic currents decreased and the active corroding sites were blocked completely. Moreover, a decrease in the mass of mild steel in an aggressive environment was reduced gradually with an increase in the concentration (ppm) of CdO-NPs inhibitor, resulting in an increase in the inhibition efficiency. The novel synthesized CdO-NPs were characterized by FT-IR, XRD and SEM-EDX spectroscopy.

1. Introduction

In recent times, acids have found different roles in various industries such as refining crude oil, pickling, cleaning, and acid scaling.[1,2] Amongst various commercial acids used, hydrochloric acid is the most frequently used acid in the oil and gas industry due to its high solubility in water. It removes scale, rust, and carbonite deposits.[3–5] The major disadvantage of hydrochloric acid is that it causes corrosion of metals and their alloys.[6,7] Corrosion has become a worldwide problem causing a huge destruction of life and property. Hence, in the last few decades, untiring efforts and attempts have been made to discover novel, economical, efficient, eco-friendly methods to eradicate and reduce corrosion. The use of corrosion inhibitors is one of the convenient methods to protect the metal. A corrosion inhibitor is a substance when added in low quantities to a corrosive environment, effectively reduces the corrosion of metal in an acidic medium.[8–10] It reduces the rate of metal dissolution by adsorbing ions or molecules to form a protective layer on the metal surface.[11] Different compounds such as chromates, silicates, phosphates, and arsenate-based inorganic inhibitors were tried as high-performance inhibitors due to their toxic nature, and their application has been restricted by various environmental laws.[12] Synthetic organic inhibitors were also developed and tried but their high toxicity and manufacturing cost have restricted their usage.[13] Hence, researchers started focusing on eco-friendly, inexpensive, and biodegradable corrosion inhibitors.[14,15] This led to the concept of green inhibitors, which offer numerous benefits such as high accessibility, easy production, renewability, and more efficiency.[16,17] Corrosion inhibitive property of plant extracts is attributed to the electro-active organic functional groups such as amine, hydroxyl, and carboxyl, or compounds containing functional groups such as phenols in the phytochemical extract. These compounds contain electro-active atoms such as nitrogen, oxygen, and sulfur as well as C–C bonds with π electrons interacting with vacant d-orbitals of metals.[17,18] In this research work, the leaf extract of Syzygium cumini (Java plum) was used, which is a potential natural corrosion inhibitor. In the experimental work, Syzygium cumini is preferred because of its biodegradability and high solubility in water. It is an evergreen tropical tree in the family of Myrtaceae. It is mostly present in the region of South America and Southeast Asia.[19] Most of the plant part is associated with multiple applications such as food, medicine, and furnishings.[20] However, without any effective use, the leaves are usually discarded as waste. Java plum leaves have a high amount of ferulic acid, rutin, catechin, and limonene.[21] Nanoparticles are extensively used in various fields due to their exceptional characteristic features.[22,23] However, the cost factor and eco-friendly aspects are the biggest concerns in green synthesis. In recent years, seeds, leaves, barks, plant biomass and micro-organisms have become the economical and eco-friendly solutions to synthesize nanoparticles.[24] Plant-based nanoparticle synthesis has a number of advantages over other methods, including ease of preparation, processing, cost-effectiveness, rapid development, reproducible, stable components, environmental friendliness, and the avoidance of

[a]*Vel TechRangarajan Dr. Sagunthala R&D Institute of Science and Technology, Avadi, Chennai 600062, India. E-mail: drgayathrij@veltech.edu.in; drsivakumars@veltech.edu.in*
[b]*Kristu Jayanti College (Autonomous), Bangalore, India*
[c]*Rajalakshmi Engineering College, Thandalam, Chennai 602 105, India*

harsh and toxic chemicals. Furthermore, the particle size is influenced by compounds such as phenols and polyphenols in the leaf extract, which play a crucial role in the reduction of ions to form stable NPs.[25] There is a significant variation in the chemical compositions of plant extract of the same species when it is collected from different parts of the world and which may lead to different results. So, these results indicate that there is a need for an in-depth study of the compounds present in the plant materials that play a crucial role in the synthesis of NPs.[23]

In the present work, we have synthesized cadmium oxide nanoparticles (CdO NPs) using the aqueous extract of Syzygium cumini leaves as a reducing agent at room temperature. Then, the characterization of CdO NPs was performed using several techniques such as XRD, FTIR, and SEM-EDX spectroscopy. Most industrial machine parts are made from mild steel, and many industries maintain machinery parts for cleaning processes such as descaling and acid pickling. To overcome the drawbacks, our research team decided to prefer CdO NPs to form a complex as it is less toxic compared with other metal oxides and also eco-friendly to our environment Also, an attempt has been made to find the corrosion resistance ability of CdO-NPs layer formed on mild steel substrate in the acidic medium. Corrosion techniques such as potentiodynamic polarization (PDP) and electrochemical impedance spectroscopy (EIS) were used to study the corrosion resistance ability.

2. Materials and methods

2.1 Chemicals and instrumentation

Sulphuric acid (32%), sodium hydroxide, acetone and ethanol were purchased from Merck Chemicals. $Cd(NO_3)_2 \cdot 6H_2O$ was commercially obtained from Sigma-Aldrich Chemicals, India, and diluted with distilled water to prepare 0.5 M H_2SO_4 solution, used as a corrosion inhibitor. The study investigated the structural morphology of pellets made with a CdO-Syzygium cumini complex and KBr using FTIR and XRD techniques. The XRD patterns were recorded using a Rigaku Maniflex diffractometer and JSM-6390 Scanning Electron Microscope. The EIS and potentiodynamic polarization were analyzed with an EC-LAB 10.37 model instrument with a cell of three-electrode system. The mild steel was used as the working electrode, the platinum electrode was used as the counter electrode, and SCE as the reference electrode. The open circuit potential OCP was stabilized up to 1800 s by keeping the scan rate at 0.5 mV s^{-1}, and potentiodynamic polarization plots were observed for the applied potential value between −200 mV and +200 mV. Electrochemical impedance spectroscopy (EIS) was performed in the frequency range of 100 kHz to 10 mHz AC sine wave possessing 10 mV amplitude. The weight loss method was used for studying corrosion inhibition efficiency.

2.2 Preparation of aqueous leaf extract of syzygium cumini (java plum)

Syzygiumn cumini leaves were collected from Vel Tech University, Chennai, India. The leaves were washed several times with double distilled water to remove the impurities. Note that 10 g of leaves was soaked with 100 mL of boiled DD water for 30 min. The boiled leaves solution changes from colourless to brown colour. Then, the leaf extract was filtered using Whatman grade No. 1 filter paper. The filtrate was centrifuged at 7500 rpm for 5 min. The aqueous leaf extract was used for further analysis.[26]

2.3 Green synthesis of cadmium oxide nanoparticles (CdO-NPs)

The study involved adding 20 mL of Syzygium cumini leaf extract to 200 mL of 0.1 M cadmium nitrate solution maintained at room temperature. The reaction solution was further heated on a hot plate at 60 °C for 2 h with a continuous magnetic stirrer. Afterward, 1.0 M of NaOH was added to the solution to maintain the pH at 10.0 until a grayish-green powder was obtained. The solution was allowed to cool and centrifuged at 8000 rpm for 10 min. The precipitate formed was maintained at 200 °C in a hot air oven for 2 h. Then, the resulting powder samples were used for further characterization, revealing the formation of cadmium oxide nanoparticles (CdO-NPs).[27] The formation of green synthesized cadmium oxide nanoparticles is shown in Scheme 1.

2.4 Surface pretreatment of a mild steel electrode

The Mild Steel (MS) electrode (percentage by weight) consisted of C: 0.21%, Si: 0.035%, Mn: 0.25%, P: 0.082% and Fe: 99.28% used for corrosion studies. The mild steel electrode, having 4 cm × 2 cm × 0.2 cm in sizes, abrades with disparate grade (600, 800 up to 1200) and the exposed surface area was 1 cm^2. Subsequently, the surface of the electrode was washed under running water and degreased in ethanol, acetone, and desiccated. With recently polished coupons, gravimetric measurements to gauge reluctance were carried out.[28–33]

2.5 Preparation of hostile solutions

The aggressive solution (0.5 M) for metal dwindling was prepared by diluting AR-grade sulphuric acid, while inhibition measurements were performed by adding CdO-NPs (100 ppm to 500 ppm) to the hostile solutions.

3. Results and discussion

3.1 FTIR analysis of CdO-NPs

The synthesis of CdO-NPs was confirmed by Fourier transform infrared spectroscopy (FT-IR spectrum). Fig. 1 reveals the spectrum recorded in the range of 400–4000 cm^{-1}. The FT-IR spectrum of CdO-NPs showed a broad absorption band at 3435 cm^{-1} for hydroxyl ions and 2040 cm^{-1} for aliphatic –CH_2– whereas carbonyl stretching was observed at 1700–1642 cm^{-1}. The bands at 1444 cm^{-1} and 1072 cm^{-1} indicate the presence of N=C and C–O bands, respectively. The FT-IR band at 670 cm^{-1} is attributed to the stretching band of cadmium oxide.

3.2 XRD analysis of CdO-NPs

The formation of the CdO-NP composite was characterized by XRD analysis. Fig. 2 demonstrates the X-ray diffraction pattern

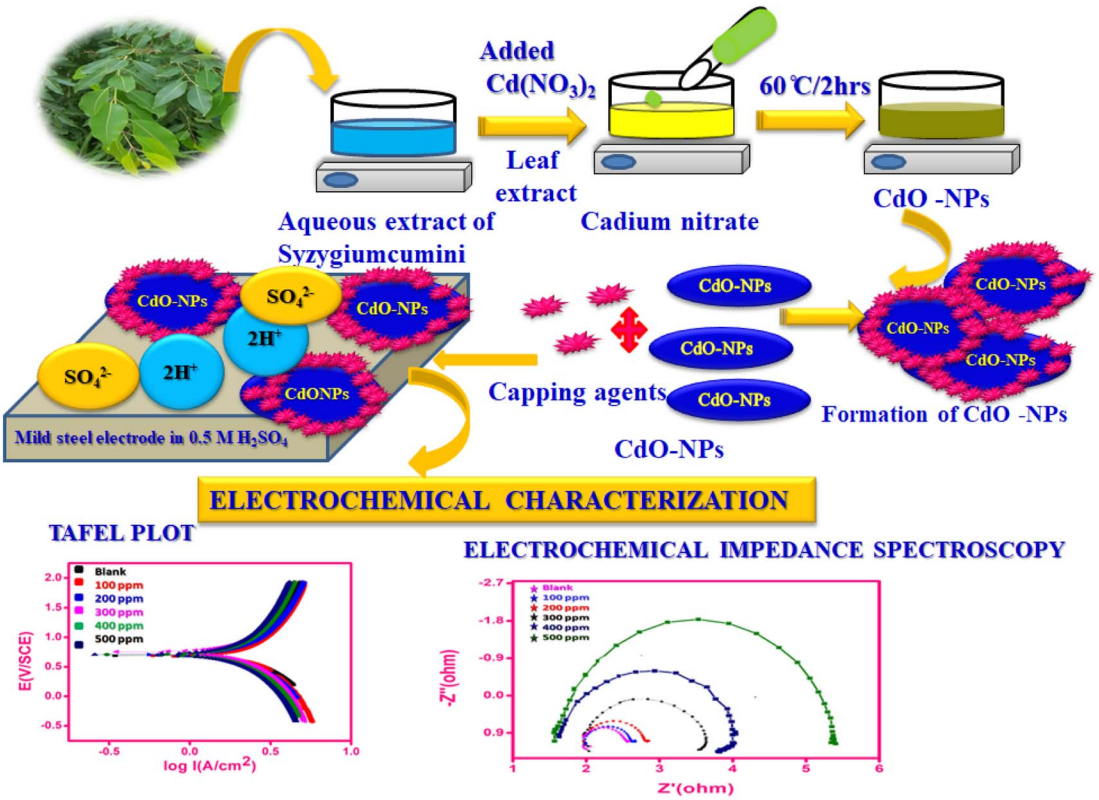

Scheme 1 The mechanism for the formation of green synthesized cadimum oxide nanoparticles.

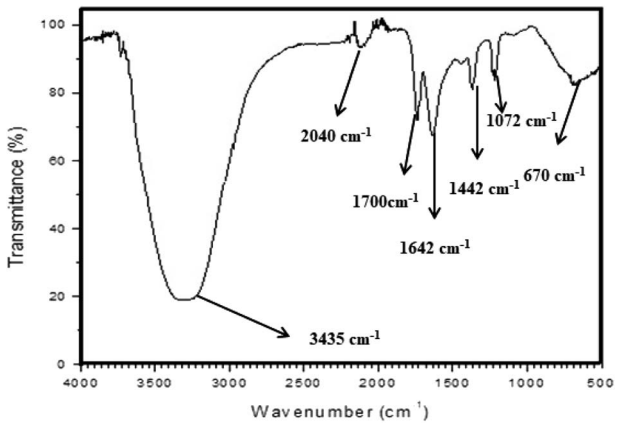

Fig. 1 FT-IR spectra of CdO-NPs.

of CdO-NPs.[33–35] The characteristic peak of CdO-NPs observed at plane values of (100), (110) and (214), which correspond to the cubic phase with $a = 0.465$ nm (JCPDS Card No: 75-0592).

The crystallite size (D) was calculated using Debye–Scherrer's formula shown in eqn (1).

$$D = k/\beta\cos\theta \quad (1)$$

where λ is the wavelength of X-ray (1.5406 Å), k is a constant (0.94), β is full width at half maximum (FWHM) and θ is the glancing angle. The average crystallite size (D) is 24 nm.

3.3 SEM with EDX analysis of CdO-NPs

Fig. 3A shows SEM analysis of CdO-NPs that revealed a granular structure with a diameter of 49.84 nm to 72.06 nm, with slight modifications in the synthesis and EDX analysis indicating a protective layer, in the aggressive environment.[23,27,28,33]

3.4 Exploration of the inhibition property

3.4.1 Corrosion measurements. The study evaluates the impact of aggressive environments on mild steel surfaces by assessing weight loss in blank and test solutions. Corroded steel is cleaned acetone, dried and reweighed to determine the inhibition efficacy (IE%) and surface coverage (θ). The results are presented in Table 1.[36]

$$\%\text{Efficiency} = \frac{W_o - W_i}{W_o} \times 100 \quad (2)$$

where W_i and W_o are weight loss values (g) on mild steel in 0.5 M H_2SO_4 with and without CdO-NPs, respectively (Fig. 4).[36]

The corrosion rate (CR) of mild steel was calculated using the relationship in eqn (3).

$$\text{CR}\%(\text{mmpy}) = \frac{KW}{AtD} \quad (3)$$

where W is the weight loss of mild steel (mg), A is the area of the mild steel (cm^2), t is the exposure time (h) and D is the density of mild steel (g cm^{-3}).

$$\text{Inhibition efficiency } (\%) = \text{CR}_B - \text{CR}_I/\text{CR}_B \times 100 \quad (4)$$

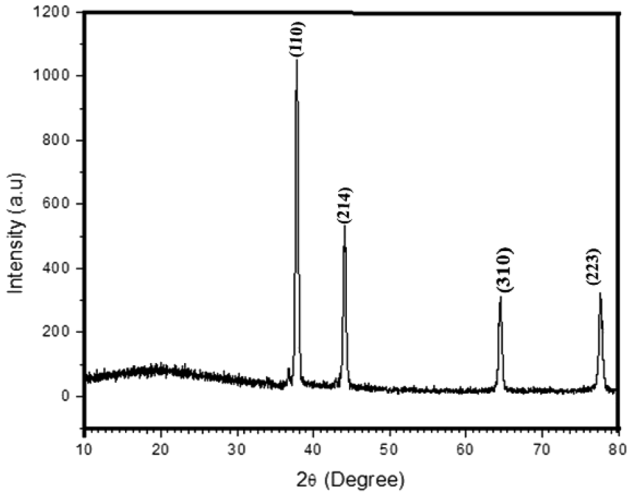

Fig. 2 XRD patterns of CdO-NPs.

where CR_B and CR_I are the corrosion rate of mild steel in the presence and absence of inhibitors in eqn (4).

According to the information in the above table, CdO-NPs are capable of protecting against 0.5 M acidic solution with a 91% efficacy with 500 ppm of the inhibitor solution at 2 h and 87% efficiency at 8 h. The above results suggested that cleaning agents with an acid concentration of less than or equal to 0.5 M could be added to the CdO-NPs combination.[28,37]

3.4.2 Potentiodynamic polarization studies. Fig. 5 shows the Tafel plot for CdO-NPs adsorbed on mild steel in 0.5 M sulphuric acid test solution for different concentrations (100 ppm to 500 ppm). The cathodic and anodic polarization curves were deduced to determine the corrosion current density (I_{corr}) using corrosion potential (E_{corr}). The values obtained from the plot of corrosion potential and corrosion current density are provided in Table 2. From the eqn (5), the percentage efficiency (η%) was calculated. The η% was increased by increasing the concentration of the inhibitor from 100 to 500 ppm. Therefore, the results reveal 79% to 91% efficiency, which indicates that the CdO-NPs have a good absorption behavior on mild steel in a corrosive environment. The values of polarization resistance increase and corrosion current (I_{corr}) decrease substantially (0.1036 μA cm^{-2} to 0.0097 μA cm^{-2}). Therefore, it can be concluded that CdO-NPs adsorbed on the surface of the mild steel exhibit an excellent corrosion resistance performance in an extremely aggressive acidic medium. From Table 2, the documented values of the electrochemical parameters such as R_p, β_a, β_c, E_{corr}, I_{corr}, C. Rate mm $year^{-1}$, (η%) percentage efficiency, and surface coverage area (θ) were obtained from the corrosion process; moreover, the calculation of inhibition efficacy, η, was performed using eqn (5):

$$\%\ \eta\ \text{Efficiency} = \frac{I^0_{corr} - I^0_{corr}}{I^0_{corr}} \times 100 \quad (5)$$

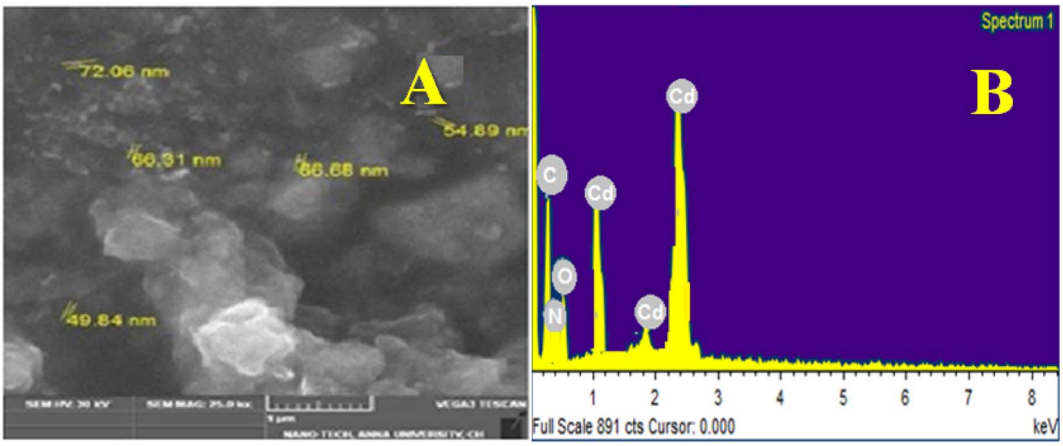

Fig. 3 SEM Image and EDX of CdO-NPs.

Table 1 The values of IE and θ were determined from weight loss measurements in 0.5 M blank and test solutions

Conc. of inhibitor solution (ppm)	2 hours			4 hours			6 hours			8 hours		
	CR mm py	I.E (%)	(θ)	CR mm py)	I.E (%)	(θ)	CR mm py)	I.E (%)	(θ)	CR mm py	I.E (%)	(θ)
Blank	99.67	—	—	82.821	—	—	69.945	—	—	65.81	—	—
100	13.861	86	0.8609	12.956	86	0.8608	12.121	83	0.8267	12.085	81	0.8163
200	12.189	88	0.8777	11.427	86	0.8620	11.308	84	0.8383	10.971	83	0.8332
300	11.354	89	0.8870	10.866	87	0.8687	10.774	85	0.8459	10.744	84	0.8367
400	9.891	90	0.9013	9.562	88	0.8847	8.3355	88	0.8802	10.256	84	0.8441
500	8.707	91	0.9124	8.185	90	0.9011	7.2910	89	0.8957	8.6370	86	0.8687

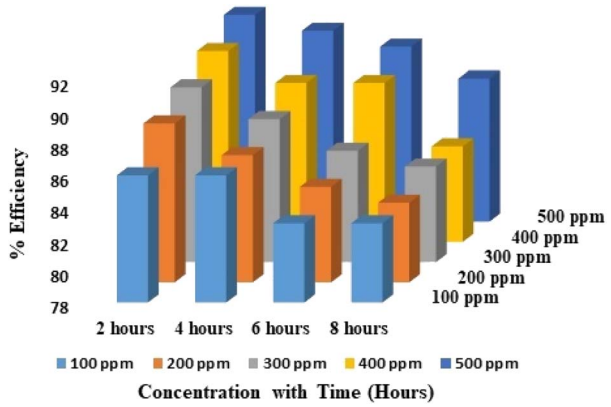

Fig. 4 Inhibition efficiency portrayal by bar chart for 0.5 M test solution.

In the above equation, $I_{corr}{}^{0}$ and I_{corr} are corrosion current densities in the absence and presence of inhibitors.[38–41]

3.4.3 Electrochemical impedance spectroscopy (EIS) measurements. According to the impedance spectra data, the impedance curve and Bode plots shown in Fig. 6A and B, respectively, were obtained when mild steel was dissolved in 0.5 M H_2SO_4 without the presence of an inhibitor and at different concentrations of the CdO-NPs. It is evident that the addition of an inhibitor to an aggressive solution causes a significant alteration in the inhibition property of mild steel. Close analysis reveals that, in the inhibitor solution, the semi-circles' diameter is larger than what it is in the inhibitor-free solution. The CdO-NPs inhibitor gets adsorbed over the metal surface and inhibits the flow of corrosion current, acting as a particularly effective inhibitor in very low pH environments. This is due to the increase in the capacitive loop size with an increase in inhibitor concentration. As stated in the impedance results shown in Table 3, the value of the double-layer capacitance (C_{dl}) decreases, and the charge transfer resistance (R_{ct}) value rises as the CdO-NPs inhibitor concentration increases.

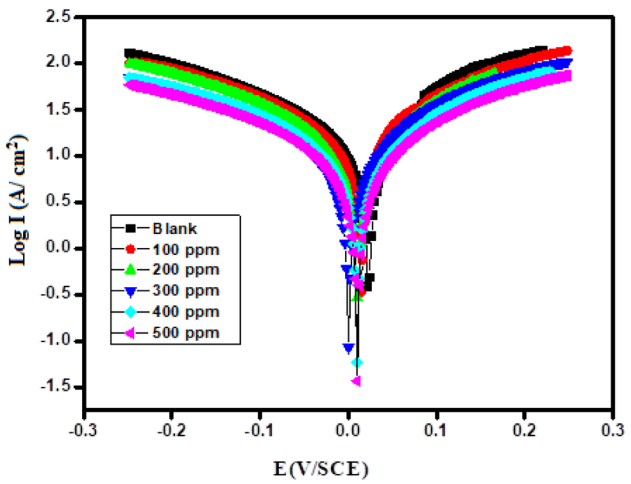

Fig. 5 Potentiodynamic polarization curve of mild steel in 0.5 M blank and test solutions.

Table 2 Corrosion resistive parameters in 0.5 M H_2SO_4 and test solution

Conc. Of inhibitor (ppm)	$-E_{corr}$ (mV *vs.* SCE)	R_P (Ω)	β_a (mV dec^{-1})	β_c (mV dec^{-1})	I_{corr} (μA cm^{-2})	C-rate (mm year^{-1})	Inhibition efficiency (η%)	Surface coverage (θ)
Blank	0.443	3.018	0.116	0.250	0.1036	229.8	00	00
100	0.014	3.303	0.275	0.296	0.0217	160.3	79	0.7905
200	0.027	3.327	0.164	0.286	0.0131	157.2	87	0.8735
300	0.009	4.585	0.239	0.300	0.0121	141.1	88	0.8832
400	0.090	4.750	0.219	0.296	0.0114	133.5	89	0.8899
500	0.006	5.837	0.240	0.290	0.0097	114.1	91	0.9063

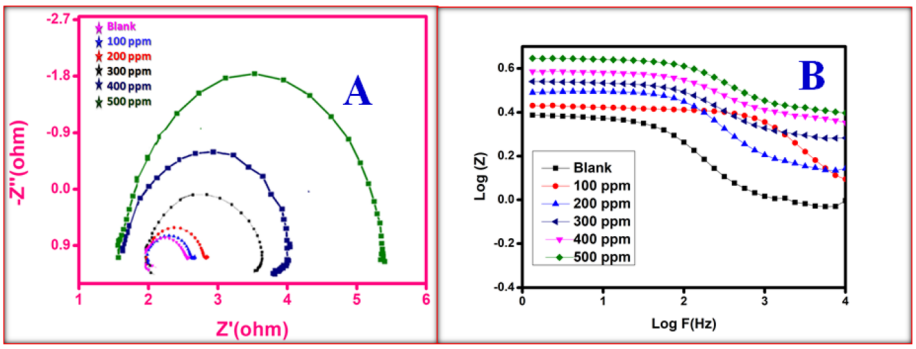

Fig. 6 Impedance plot for mild steel in 0.5 M blank and test solution (A) and (B) Bode plots.

Table 3 Impedance parameters derived for 0.5 M blank and test solution

Conc. of inhibitor (ppm)	R_s (Ω)	C_{dl} (μF cm^{-2})	R_{ct} (Ω cm^2)	Inhibition efficiency (%)	Surface coverage (θ)
Blank	1.78	5.36	0.5071	00	00
100	1.41	4.12	0.99	49	0.4877
200	1.57	3.47	1.21	58	0.5809
300	1.51	3.12	2.05	75	0.7526
400	2.62	1.98	3.25	84	0.8439
500	2.41	1.87	4.95	90	0.8976

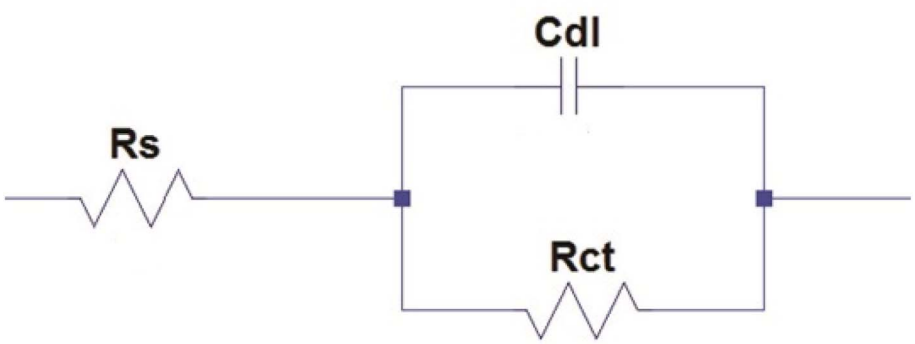

Fig. 7 Electrical equivalent circuit diagram.

The results of EIS parameters such as charge transfer resistance (R_{ct}) and double layer capacitance (C_{dl}) were determined using the following electrical equivalent circuit diagram as depicted in Fig. 7.[22,41] The percentage efficiency (η) was calculated using eqn (6).

$$\%\eta \text{ Efficiency} = \frac{R_{ct} - R_{ct}^{0}}{R_{ct}} \times 100 \quad (6)$$

In the above equation, R_{ct}^{0} and R_{ct} are the charge transfer resistance of the blank and the inhibitor solution, respectively.

4. Conclusions

The anti-corrosive electrochemical performance of green synthesized CdO-NPs as corrosion inhibitors on mild steel in a low pH environment was evaluated. The percentage inhibition efficiency of 87% was observed even with an immersion time of up to 8 h and 91% for 2 h using the weight loss method and it increased with surface coverage area. The potentiodynamic polarization study presented a 91% efficacy 500 ppm test solution. The CdO-NPs system worked mostly as a mixed type of inhibitor. The electrochemical impedance measurements indicated that owing to the engorged thickness of the surface layer on the mild steel surface, an increase in R_{ct} value and a decrease in C_{dl} and I_{corr} values due to charge transfer were observed. Therefore, the result revealed that the inhibitor material forms a defensive barrier film on the mild steel surface. Moreover, there was an increasing trend of the safeguard efficiency with respect to the increase in the concentration of the inhibitor (100 ppm to 500 ppm) observed in weight loss, and PDP and EIS studies implies that the water-soluble inhibitor material can act

as a good protecting agent during the industrial cleaning, pickling and descaling process.

Conflicts of interest

There are no conflicts to declare.

Acknowledgements

The authors are thankful to the Dean R and D and University Management Committee Members of Vel Tech Rangarajan Dr. Sagunthala R and D Institute of Science and Technology, Avadi, Chennai. for providing necessary instrumental facilities to carry out research work.

References

1 P. S. Neriyana and V. D. Alva, A green approach: evaluation of *Combretum indicum* (CI) leaf extract as an eco-friendly corrosion inhibitor for mild steel in 1M HCl, *Chem. Afr.*, 2020, **3**(4), 1087–1098.

2 A. Salmasifar, M. Edraki, E. Alibakhshi, B. Ramezanzadeh and G. Bahlakeh, Combined electrochemical/surface investigations and computer modeling of the aquatic Artichoke extract molecules corrosion inhibition properties on the mild steel surface immersed in the acidic medium, *J. Mol. Liq.*, 2021, **327**, 114856.

3 S. Prifiharni, G. Mashanafie, G. Priyotomo, A. Royani, A. Ridhova, B. Elya and J. W. Soedarsono, Extract sarampa wood (Xylocarpus Moluccensis) as an eco-friendly corrosion inhibitor for mild steel in HCl 1M, *J. Indian Chem. Soc.*, 2022, **99**(7), 100520.

4 B. N. Abba, R. Idouhli, A. T. Ilagouma, A. Abouelfida, M. Khadiri and A. Romane, Use of Endostemon tereticaulis (Pear.) M. Ashby and *Hyptis spicigera* Lam. plant extracts as corrosion green inhibitors for mild steel in 1M HCl: electrochemical and surface morphological studies, *Protect. Met. Phys. Chem. Surf.*, 2021, **57**, 619–633.

5 J. P. Rajan, R. Shrivastava and R. K. Mishra, Corrosion inhibition effect of clerodendron colebrookianum Walp leaves (Phuinam) extract on the acid corrosion of mild steel, *Protect. Met. Phys. Chem. Surf.*, 2017, **53**, 1161–1172.

6 X. Sun, Y. Qiang, B. Hou, H. Zhu and H. Tian, Cabbage extract as an eco-friendly corrosion inhibitor for X70 steel in hydrochloric acid medium, *J. Mol. Liq.*, 2022, **362**, 119733.

7 A. S. Fouda, G. Y. El-Awady and W. T. El Behairy, *Prosopis juliflora* plant extract as potential corrosion inhibitor for low-carbon steel in 1 M HCl solution, *J. Bio Tribo Corros.*, 2018, **4**, 1–2.

8 S. Perumal, S. Muthumanickam, A. Elangovan, R. Karthik, R. S. Kannan and K. K. Mothilal, Bauhinia tomentosa leaves extract as green corrosion inhibitor for mild steel in 1 M HCl medium, *J. Bio Tribo Corros.*, 2017, **3**, 1.

9 A. A. Khadom, A. N. Abd, N. A. Ahmed, M. M. Kadhim and A. A. Fadhil, Combined influence of iodide ions and *Xanthium strumarium* leaves extract as eco-friendly corrosion inhibitor for low-carbon steel in hydrochloric acid, *Curr. Res. Green Sustainable Chem.*, 2022, **5**, 100278.

10 F. A. Zakaria, T. S. Hamidon and M. H. Hussin, Applicability of winged bean extracts as organic corrosion inhibitors for reinforced steel in 0.5 M HCl electrolyte, *J. Indian Chem. Soc.*, 2022, **99**(2), 100329.

11 N. Raghavendra, Latest exploration on natural corrosion inhibitors for industrial important metals in hostile fluid environments: a comprehensive overview, *J. Bio Tribo Corros.*, 2019, **5**(3), 54.

12 A. Dehghani, P. Ghahremani, A. H. Mostafatabar and B. Ramezanzadeh, Plant extracts: probable alternatives for traditional inhibitors for controlling alloys corrosion against acidic media—A review, *Biomass Convers. Biorefin.*, 2022, 1–20.

13 J. Panchal, D. Shah, R. Patel, S. Shah, M. Prajapati and M. Shah, Comprehensive review and critical data analysis on corrosion and emphasizing on green eco-friendly corrosion inhibitors for oil and gas industries, *J. Bio Tribo Corros.*, 2021, **7**(3), 107.

14 N. Chaubey, A. Qurashi, D. S. Chauhan and M. A. Quraishi, Frontiers and advances in green and sustainable inhibitors for corrosion applications: a critical review, *J. Mol. Liq.*, 2021, **321**, 114385.

15 D. S. Chauhan, M. A. Quraishi and A. Qurashi, Recent trends in environmentally sustainable Sweet corrosion inhibitors, *J. Mol. Liq.*, 2021, **326**, 115117.

16 Y. Fang, B. Suganthan and R. P. Ramasamy, Electrochemical characterization of aromatic corrosion inhibitors from plant extracts, *J. Electroanal. Chem.*, 2019, **840**, 74–83.

17 A. S. Fouda, O. A. Mohamed and H. M. Elabbasy, Ferula hermonis plant extract as safe corrosion inhibitor for zinc in hydrochloric acid solution, *J. Bio Tribo Corros.*, 2021, **7**(4), 135.

18 J. Lohitkarn, P. Hemwech, R. Chantiwas and M. Jariyaboon, The role of cassava leaf extract as green inhibitor for controlling corrosion and scale problems in cooling water systems, *J. Failure Anal. Prevent.*, 2021, **21**, 847–860.

19 H. Ma, N. J. Kabengi, P. M. Bertsch, J. M. Unrine, T. C. Glenn and P. L. Williams, Comparative phototoxicity of nanoparticulate and bulk ZnO to a free-living nematode *Caenorhabditis elegans*: the importance of illumination mode and primary particle size, *Environ. Pollut.*, 2011, **159**(6), 1473–1480.

20 T. M. Bandiola and M. J. Corpuz, Platelet and leukocyte increasing effects of *Syzygium cumini* (L.) skeels (*Myrtaceae*) leaves in a murine model, *Pharm Anal Acta*, 2018, **9**(05), 1–6.

21 R. Riastuti, G. Mashanafie, V. Rizkia, A. Maksum, S. Prifiharni, K. Agus Paul Setiawan, G. Priyotomo and J. W. Soedarsono, Effect of syzygium cumini leaf extract as a green corrosion inhibitor on API 5l carbon steel in 1M HCL, *East. Eur. J. Enterprise Technol.*, 2022, **6**(6), 120.

22 M. C. Daniel and D. Astruc, Gold nanoparticles: assembly, supramolecular chemistry, quantum-size-related properties, and applications toward biology, catalysis, and nanotechnology, *Chem. Rev.*, 2004, **104**(1), 293–346.

23 S. A. Khan, M. Zahera, I. A. Khan, M. S. Khan, A. Azam, M. Arshad, A. Syed, O. Nasif and A. M. Elgorban, Photocatalytic degradation of methyl orange by cadmium oxide nanoparticles synthesized by the sol-gel method, *Optik*, 2022, **251**, 168401.

24 K. Kalishwaralal, V. Deepak, S. R. Pandian, M. Kottaisamy, S. BarathManiKanth, B. Kartikeyan and S. Gurunathan, Biosynthesis of silver and gold nanoparticles using *Brevibacterium casei*, *Colloids Surf., B*, 2010, **77**(2), 257–262.

25 B. D. Lade and A. S. Shanware, Phytonanofabrication: methodology and factors affecting biosynthesis of nanoparticles, in *InSmart Nanosystems for Biomedicine, Optoelectronics and Catalysis*, IntechOpen, 2020.

26 M. Arumugam, D. B. Manikandan, E. Dhandapani, A. Sridhar, K. Balakrishnan, M. Markandan and T. Ramasamy, Green synthesis of zinc oxide nanoparticles (ZnO NPs) using *Syzygium cumini*: potential multifaceted applications on antioxidants, cytotoxic and as nanonutrient for the growth of *Sesamum indicum*, *Environ. Technol. Innovat.*, 2021, **23**, 101653.

27 M. El-Kemary, N. Nagy and I. El-Mehasseb, Nickel oxide nanoparticles: synthesis and spectral studies of interactions with glucose, *Mater. Sci. Semicond. Process.*, 2013, **16**(6), 1747–1752.

28 G. Subramanian, R. S. Kannan, M. Malarvizhi and P. Muthirulan, A novel eco-friendly corrosion inhibitor for mild steel protection in two different aggressive artificial corrosive medium, *J. Chem. Pharm. Res.*, 2018, **10**, 155–163.

29 P. Shanthy, J. A. Thangakani, S. Karthika, S. C. Joycee, S. Rajendran and J. Jeyasundari, Corrosion inhibition by an aqueous extract of ervatamia divaricata, *Int. J. Corros. Scale Inhib.*, 2021, **10**(1), 331–348.

30 M. Barrahi, H. Elhartiti, A. El Mostaphi, *et al.*, Corrosion inhibition of mild steel by Fennel seeds mill (*Foeniculum vulgare*) essential oil in 1 M hydrochloric acid solution, *Int. J. Corros. Scale Inhib.*, 2019, **8**(4), 937–953, DOI: **10.17675/2305-6894-2020-10-4-10**.

31 P. Mahalakshmi, S. Rajendran, G. Nandhini, S. C. Joycee, N. Vijaya, T. Umasankareswari and D. N. Renuga, Inhibition of corrosion of mild steel in sea water by an aqueous extract of turmeric powder, *Int. J. Corros. Scale Inhib.*, 2020, **9**(2), 706–725.

32 W. M. Ikhmal, M. Y. Yasmin, M. F. Maria, S. M. Syaizwadi, W. A. Rafizah, M. G. Sabri and B. M. Zahid, Evaluating the performance of andrographis paniculata leaves extract as additive for corrosion protection of stainless steel 316l in seawater, *Int. J. Corros. Scale Inhib.*, 2020, **9**(1), 118–133.

33 S. Shunmugaperumal, P. K. Selvaraj and S. Sivalingam, Water soluble CdO-PANI composite as corrosion resistive delegate in acidic abode for mild steel, *Egpt. J. Chem.*, 2022, **65**(13), 291–299.

34 S. Rajaboopathi and S. Thambidurai, Heterostructure of CdO-ZnO nanoparticles intercalated on PANI matrix for better thermal and electrochemical performance, *Mater. Sci. Semicond. Process.*, 2017, **59**, 56–67.

35 A. S. Roy, K. R. Anilkumar and M. V. N. Ambika Prasad, Studies of AC conductivity and dielectric relaxation behavior of CdO-doped nanometricpolyaniline, *J. Appl.*, 2012, **123**(4), 1928–1934, DOI: **10.1002/app.34696**.

36 T. Raja, S. S. Abuthahir and K. Vijaya, Anticorrosion Performance of Syzygium Cumini Leaves Extract for Carbon Steel Immersed in a Hydrochloric Acid Medium, *Port. Electrochim. Acta*, 2024, **42**, 173–189.

37 A. Singh and M. A. Quraishi, The extract of Jamun (*Syzygium cumini*) seed as green corrosion inhibitor for acid media, *Res. Chem. Intermed.*, 2015, **41**, 2901–2914.

38 Z. M. Alamshany and A. A. Ganash, Synthesis, characterization, and anti-corrosion properties of an 8-hydroxyquinoline derivative, *Heliyon*, 2019, **5**(11), e02895.

39 B. K. Liao, R. X. Quan, P. X. Feng, H. Wang, W. Wang and L. Niu, Carbon steel anticorrosion performance and mechanism of sodium lignosulfonate, *Rare Met.*, 2024, **43**(1), 356–365.

40 B. Liao, Z. Luo, S. Wan and L. Chen, Insight into the anti-corrosion performance of Acanthopanax senticosus leaf extract as eco-friendly corrosion inhibitor for carbon steel in acidic medium, *J. Ind. Eng. Chem.*, 2023, **117**, 238–246.

41 B. Liao, S. Ma, S. Zhang, X. Li, R. Quan, S. Wan and X. Guo, Fructus cannabis protein extract powder as a green and high effective corrosion inhibitor for Q235 carbon steel in 1 M HCl solution, *Int. J. Biol. Macromol.*, 2023, **239**, 124358.